Renato S. M. Almeida, Yang Li, Benjamin Besser, Peng Xiao, Wei Zhou, Alexander Brückner, Nico Langhof, Kamen Tushtev, Walter Krenkel, Kurosch Rezwan

Damage analysis of 2.5D C/C-SiC composites subjected to fatigue loadings

Journal Article as: peer-reviewed accepted version (Postprint)

DOI of this document*(secondary publication): 10.26092/elib/2618

Publication date of this document: 27/10/2023

* for better findability or for reliable citation

Recommended Citation (primary publication/Version of Record) incl. DOI:

Renato S.M. Almeida, Yang Li, Benjamin Besser, Peng Xiao, Wei Zhou, Alexander Brückner, Nico Langhof, Kamen Tushtev, Walter Krenkel, Kurosch Rezwan,
Damage analysis of 2.5D C/C-SiC composites subjected to fatigue loadings,
Journal of the European Ceramic Society, Volume 39, Issue 7, 2019, Pages 2244-2250, ISSN 0955-2219,
https://doi.org/10.1016/j.jeurceramsoc.2019.01.014

Damage analysis of 2.5D C/C-SiC composites subjected to fatigue loadings

Renato S.M. Almeida[b], Yang Li[a,*], Benjamin Besser[c], Peng Xiao[a], Wei Zhou[d], Alexander Brückner[e], Nico Langhof[d], Kamen Tushtev[b], Walter Krenkel[d], Kurosch Rezwan[b,f]

[a] Powder Metallurgy Research Institute, Central South University, 410083 Changsha, China
[b] Advanced Ceramics, University of Bremen, Am Biologischen Garten 2, 28359 Bremen, Germany
[c] Center for Environmental Research and Sustainable Technology (UFT), University of Bremen, 28359 Bremen, Germany
[d] Ceramic Materials Engineering, University of Bayreuth, 95447 Bayreuth, Germany
[e] Polymer Engineering, University of Bayreuth, 95447 Bayreuth, Germany
[f] MAPEX - Center for Materials and Processes, University of Bremen, 28359 Bremen, Germany

ARTICLE INFO

Keywords:
A. Ceramic-matrix composites (CMCs)
B. Fatigue
D. Acoustic emission
Damage threshold

ABSTRACT

Damage analyses of a ceramic matrix composite during fatigue and quasi-static loads were performed by acoustic emission (A.E.) monitoring. The material studied was a 2.5D C/C-SiC composite produced by chemical vapor infiltration followed by liquid silicon infiltration. The analysis done during the first 200 cycles of a fatigue test showed that the number of A.E. hits is a good parameter for the quantification of damage. Furthermore, the A.E. hit energy was associated with the type of damage. In this sense, the damage developed during the fatigue loading was related to matrix crack initiation, propagation and re-opening, as well as fiber-matrix friction. Quasi-static tests on post-fatigue samples showed that the previous fatigue loadings increased the material`s damage threshold and hindered the development of new damage. Particular attention was given to the sample after 2,000,000 cycles as this sample showed distinct A.E. signals that could be related to fiber debonding.

1. Introduction

Advances on the liquid silicon infiltration (LSI) processing technique allowed the relatively low-cost production of C/C-SiC composites [1]. These ceramic matrix composites (CMC) show high strength and thermal resistance, as well as quasi-plastic mechanical behavior. Therefore, C/C-SiC have gained increasing attention on aerospace applications and advanced friction systems [2,3]. In the last years, particular attention was given to C/C-SiC composites with 2.5 dimensional fiber reinforcement (2.5D C/C-SiC) for tribological applications. The combination of long and short fibers leads to a favorable balance between manufacture cost efficiency, mechanical properties (tensile strength, shear strength and toughness), good coefficient of friction and thermal properties [4,5]. The majority of recent scientific studies related to this material are focusing on production aspects, as well as its suitability for heavy-duty break systems [6–9]. However, there is still only a few works on the long-term fatigue behavior of 2.5D C/C-SiC [10,11]. For CMCs, in general, cyclic loads cause matrix cracking and fiber-matrix friction that reduces the elastic modulus of the composite. This may lead to the degradation or enhancement of post-fatigue mechanical properties of the CMC [12–14]. In the case of the 2.5D C/C-SiC, an increase of the tensile strength was seem after fatigue loading in our previous study [10]. This was related to the relief of internal stresses. Nevertheless, because of the complexity of the fiber reinforcement (see Fig. 1), it is extremely difficult to understand the occurring damage mechanisms during fatigue loading, which will also influence the post-fatigue behavior of the material.

Hence, the objective of this work is to apply acoustic emission (A.E.) monitoring on 2.5D C/C-SiC composites subjected to cyclic loads, gaining insight on the damage development caused by fatigue. During a mechanical test, A.E. signals can be related to the different mechanical responses of the tested material. This technique has been proved suitable for the damage analysis of different types of fiber-reinforced composites [15–17]. Therefore, here we use A.E. monitoring to quantify/qualify the damage of a 2.5D C/C-SiC composite during 200 fatigue cycles with maximum stress corresponding to 75% of the composite tensile strength. The damage onset for each fatigue cycle was also analyzed. Furthermore, the post-fatigue behavior was studied by performing quasi-static tensile tests on samples that were previously loaded with 200, 10,000 and 2,000,000 fatigue cycles. The mechanical behavior of the composites was also correlated to the A.E. signals measured.

* Corresponding author.
E-mail addresses: liyang_csu@126.com, liyang16@csu.edu.cn (Y. Li).

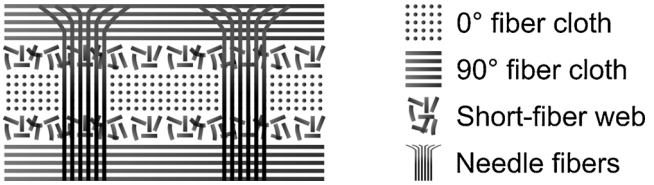

Fig. 1. Schematic representation of the 2.5D fiber reinforcement in the prepared 2.5D C/C-SiC composite.

2. Experimental

2.1. Materials

The material investigated in this work was a 2.5D C/C-SiC composite. Table 1 shows the general properties of the as-produced composite previously tested [10]. The fabrication of the 2.5D C/C-SiC composite plates consisted mainly of three steps. First, a 2.5D fiber preform was prepared by stacking short fiber webs and unidirectional fiber cloths (0° and 90°) together and, subsequently, needle-punching them (see Fig. 1). The commercially available polyacrylonitrile-based carbon fibers T700 (Toray Industries, Tokyo, Japan) with filament count of 12k were used as the raw materials. Afterward, a porous C/C composite was produced via chemical vapor infiltration (CVI) on the 2.5D fiber preforms. The process parameters used for CVI were temperature of 1000 °C with a dwell time of 100 h and absolute pressure of 0.1 MPa under argon atmosphere. C_3H_6 was applied as a precursor and H_2 as a carrier and diluting gas. Finally, the porous C/C composites, with density of 1.36 g/cm^3, were further densified via liquid silicon infiltration to prepare the 2.5D C/C-SiC composites. The LSI process was performed at 1650 °C with 0.5 h of dwell time under vacuum with absolute pressure of less than 1 Pa. The typical optical morphology of the as-prepared 2.5D C/C-SiC composite studied is presented in Fig. 2. More information about the processing of the 2.5D C/C-SiC composites was presented in our previous work [9].

2.2. Characterization methods

In this work, all specimens were machined to obtain a grinded and polished surface. For the tensile fatigue cyclic and quasi-static tensile tests, dog-bone-shaped specimens were prepared by wire eroding. The detailed geometry of the dog-bone-shaped specimen is shown in Fig. 3a. The mechanical tests were performed using a servo-hydraulic testing machine Roell-Amsler System Rel 2100 (Zwick Roell Group, Ulm, Germany) with a MTS Flex Test 40 controller (see Fig. 3b). The testing machine has an inherent position sensor, and was also equipped with a linear variable differential transformer position sensor. The applied load was measured with the 25 kN load cell of the testing machine. Strain measurements were done using a laser extensometer (Fiedler Optoelektronik GmbH, Lützen, Germany) over white marks with a distance of 25 mm between them.

To monitor the acoustic emission signals, an AMSY 4 system (Vallen Systeme GmbH, Icking, Germany) with two sensors VS 600-Z2 (400–800 kHz and Ø 4.7 mm) was used. Table 2 shows the parameters used for the acoustic emission acquisition. The threshold used was defined in order to avoid the collection of data due to noise of the machine and of friction. The sensors were attached to the sample, using hot glue, with a distance of approximately 41.5 mm between each sensor. Fig. 3b shows the arrangement used for the tests, as well as the

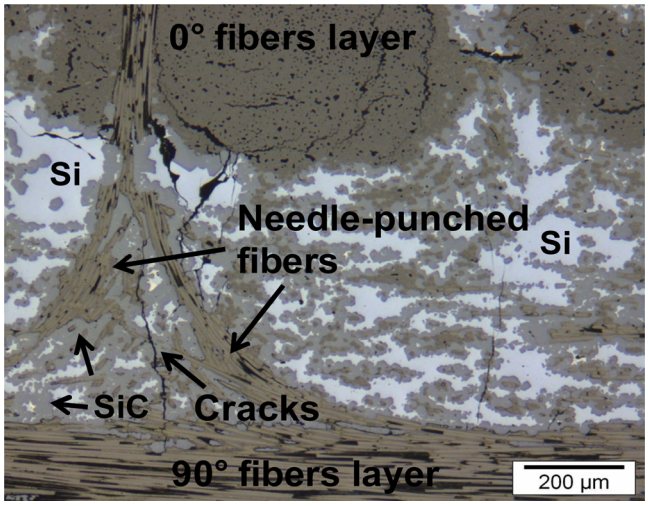

Fig. 2. Optical microstructure of the 2.5D C/C-SiC composite.

sensors. Linear location of the events was possible with the use of the two sensors. Therefore, only the signals located between the two sensors were analyzed. The following A.E. data were measured during the mechanical tests: number of hits, hit energy and damage threshold. A.E. hit energy (1 eu = 1×10^{-18} J) was calculated by integrating the values of the AE signal during the hit. By definition, damage threshold is the onset of material deterioration. In the literature, this parameter has been measured by different approaches using A.E.: Moment at which the first A.E. event happens, increase of hit energy or increase of hit count rate [15,17–19]. In order to measure the damage threshold of several loading cycles, a more automated approach was adopted. For that, the cumulative hit count *vs.* stress was analyzed. The damage threshold was then defined as the extrapolation of the linear part of the curve, as exemplified in Fig. 3c. For all samples, the linear part was considered to be the region above 50% of the total hit count.

The tensile-tensile fatigue tests were carried out in accordance to the standard ASTM C1360. A sinusoidal wave with maximum fatigue stress of 58.2 MPa, frequency of 10 Hz and fatigue stress ratio of 0.1 were used as the main parameters of the tests. The stress of 58.2 MPa (75% of the tensile strength) was determined previously as the fatigue limit considering a run-out of 10^6 cycles [10]. The dynamic modulus for each cycle was calculated by linear regression between the first and last stress/strain data point of each loading cycle. A.E. monitoring was performed on the first 200 cycles. For this analysis, only the signals that occurred during the loading cycles were considered, while the signals measured during unloading were disregarded.

Furthermore, samples that were previously fatigue loaded were characterized by quasi-static tensile tests with A.E. monitoring. The tensile tests were performed with a crosshead speed of 1 mm/min until failure, following the standard DIN EN 658-1. The specimens were analyzed after 200, 10,000 and 2,000,000 fatigue cycles and compared to the mechanical behavior of an as-produced sample. Since the emphasis in this work is mainly focused on the damage analysis under A.E. detection, and also considering the limited amount of material, only one specimen was tested for each condition.

Table 1
Properties of the 2.5D C/C-SiC composite [10].

Fiber volume fraction (%)	Bulk density (g/cm^3)	Open porosity (%)	Tensile strength (MPa)	Elastic modulus (GPa)	Fatigue limit (MPa)
30–35	2.1 ± 0.1	4.5 ± 0.5	77.7 ± 15.6	34.5 ± 7.7	58.2

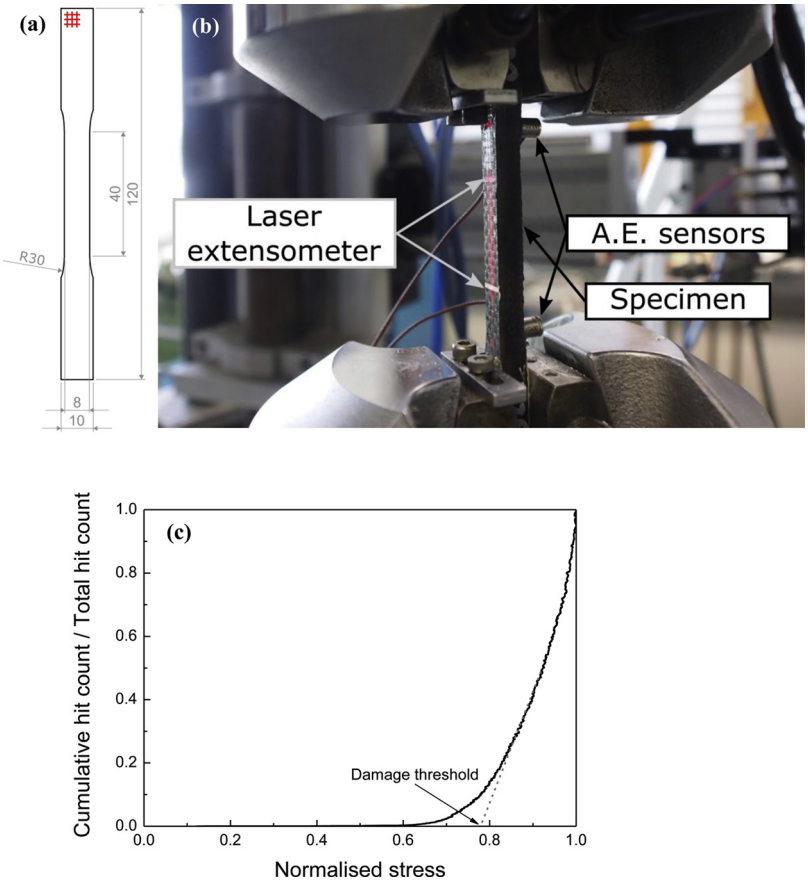

Fig. 3. (a) Geometry of the 2.5D C/C-SiC tensile specimen. (b) Servo-hydraulic testing machine equipped with laser extensometer and A.E. sensors. (c) Example curve for the determination of the damage threshold.

Table 2
Parameters for acoustic emission acquisition.

Parameter	Value
Pre-amplifier gain	34 dB
Threshold	48.6 dB
Duration discrimination time (DDT)	100 μs
Rearm time (RT)	1000 μs

3. Results

3.1. Tensile fatigue tests

Damage analysis was performed for the first 200 cycles during the fatigue test with maximum stress of 58.2 MPa. For the analysis, the following parameters were taken into consideration: dynamic modulus, A.E. hit count and A.E. hit energy. Fig. 4a shows the evolution of those parameters in relation to the number of cycles. The scales of the graph were adjusted so that the minima of the A.E. hit count and energy are coincident to the maximum of the dynamic modulus, while the maxima are coincident to the minimum. This was done for an easier comparison between the tendencies showed for each parameter. While the dynamic modulus decreases, the cumulative A.E. energy and hit count increase with the number of cycles applied. It is interesting to see that the dynamic modulus and the hit count follow a very similar trend as one curve is the inverse of the other. This indicates that the A.E. hit count is indeed a valid parameter to quantify the amount of damage during loading. In contrast, the cumulative A.E. hit energy follows a slightly different trend. Even though there is an increase of both parameters with the increase of the fatigue cycles, the evolution of both parameters is different as it can be seen that the curves do not coincide.

Further information can be obtained when analyzing the energy of each hit. Fig. 4b shows the energy of the A.E. signals measured during the loading cycles. As it can be seen, the hits of the first loading cycle have much higher energy. At the end of the first cycle, some hits reached over 500 eu. The energy of the hits measured afterwards drastically decreases. For instance, the average hit energy measured during the last 100 cycles is of only 5.5 eu. Nevertheless, a few "higher-energy" hits were also recorded at latter cycles. For instance, the 116th cycle showed a hit with 254 eu.

Another parameter measured during the fatigue test was the damage threshold, which is associated to the onset of material deterioration. Fig. 5 shows the damage threshold measured for each loading cycle. Within the first 10 cycles, the damage threshold rapidly increases. Afterwards, the damage threshold remains somewhat constant at around 56 MPa. Some scatter between the measured damage thresholds can be seen, possibly due to the lower amount of A.E. hits measured during the last cycles. Then again, some cycles after the 100th cycle showed lower damage threshold in comparison to the surrounding cycles. This is the case of the 116th cycle, which also showed hits with higher energy than the other cycles above 100 cycles (see Fig. 4b).

3.2. Quasi-static tensile tests

The post-fatigue properties of the 2.5D composite were tested with quasi-static tensile tests (see Table 3). Fig. 6 presents the elastic modulus and tensile strength of an as-produced sample, as well as samples after 200, 10,000 and 2,000,000 fatigue cycles with maximum stress of 58.2 MPa. In general, the elastic modulus decreases with the number of fatigue cycles until reaching a plateau after 10,000 cycles. On the other

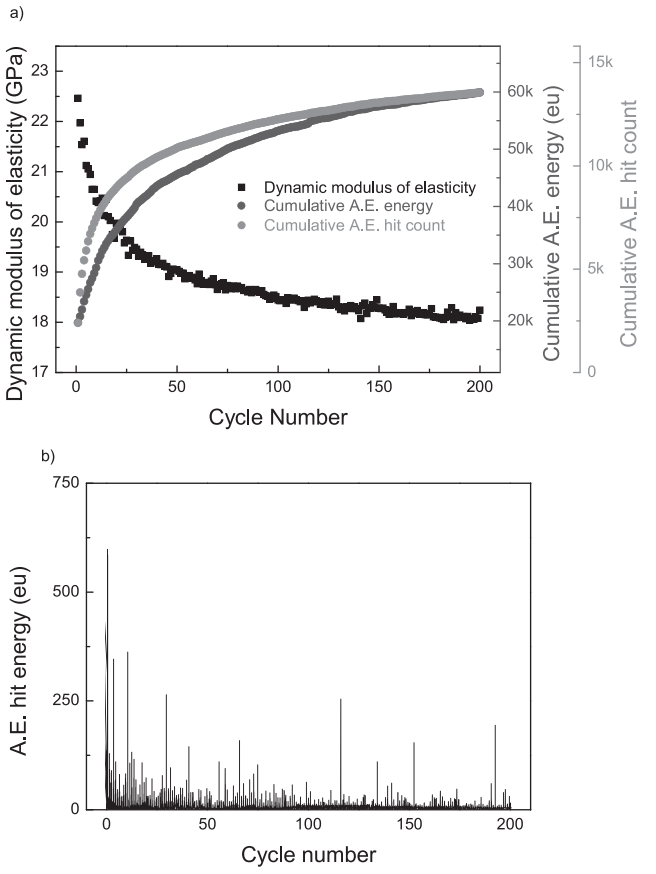

Fig. 4. Damage analysis during fatigue loading with 200 cycles and maximum stress of 58.2 MPa. (a) Evolution of dynamic modulus of elasticity, cumulative A.E. energy and cumulative A.E. hit count with the number of cycles. (b) Energy of A.E. hits measured during the loading cycles.

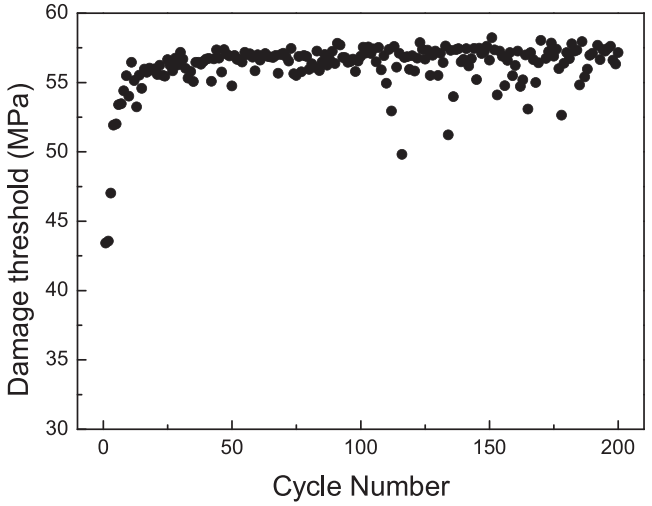

Fig. 5. Damage threshold *vs.* number of cycles for fatigue test with maximum stress of 58.2 MPa.

hand, the tensile strength increases after the fatigue loading, with the exception of the specimen previously loaded for 200 cycles. This trend is in consistence with our previous experiments [10]. However, it should be highlighted that only one sample per condition was tested in the present work. Therefore, differences with the previous results are to be considered due to the heterogeneity of the material and differences between the specimens.

Table 3
Properties measured during quasi-static loading of samples as-produced and after different fatigue loadings.

Sample	Tensile strength (MPa)	Elastic modulus (GPa)	Damage threshold (MPa)
As-produced	75.4	35.6	45.7
200 cycles	69.7	27.4	55.8
10,000 cycles	84.0	24.9	62.4
2,000,000 cycles	99.4	25.1	65.0

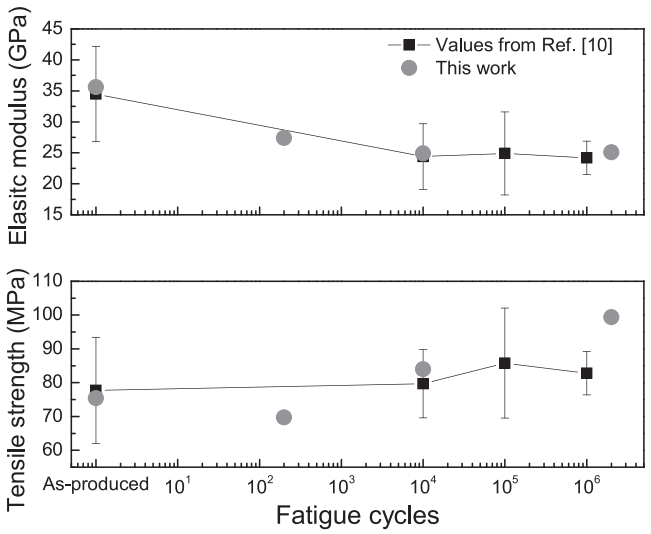

Fig. 6. Elastic modulus and tensile strength of samples after fatigue loading with max stress of 58.2 MPa.

Further effects of the previous cyclic loadings could be perceived by analyzing the fracture surface of the specimens after the quasi-static tests. Fig. 7 shows the SEM morphology of the fractured surfaces. Several fiber clusters and a few single fibers were observed along the fracture surface of the as-produced sample (Fig. 7a). In contrast, the fiber pull-out patterns for the post-fatigue specimen (Fig. 7b) are mainly composed of single fibers and small fiber bundles.

Here it is given a higher focus to the damage analysis during the post-fatigue, quasi-static tests. The stress-strain curves of the tested specimens, as well as the measured A.E. hit energy, are displayed in Fig. 8. The as-produced specimen shows a small portion of linear-elastic behavior followed by an extended non-linear region. The measured A.E. hit energy is somewhat constant on the non-linear part of the test. Still, some hits with higher energy are observed, and their energy increases at higher stresses. At the moment of failure (maximum stress), multiple hits with energy over 4000 eu were measured. These hits are outside the scale of the graph, which was adjusted for a better visualization of the lower-energy hits.

The post-fatigue samples show more linear-elastic deformation than the as-produced samples during the quasi-static tests. For the sample that underwent 200 cycles, non-linearity can still be seen before reaching the fatigue stress of 58.2 MPa. Nevertheless, the energy of the few hits measured before that is considerably low. For stresses higher than the fatigue stress, the measured A.E. hits are rather similar to the measurements on the as-produced sample. The specimens previously loaded with 10,000 and 2,000,000 cycles showed visible non-linearity only at stresses higher than 58 MPa. Above the maximum fatigue stress, each sample showed distinct behavior. The one loaded for 10,000 cycles had hits with relatively low energy, while the sample loaded for 2,000,000 cycles presented several hits with energy above 300 eu. Near to the end of the tests, all specimens showed high-energy hits like the as-produced sample.

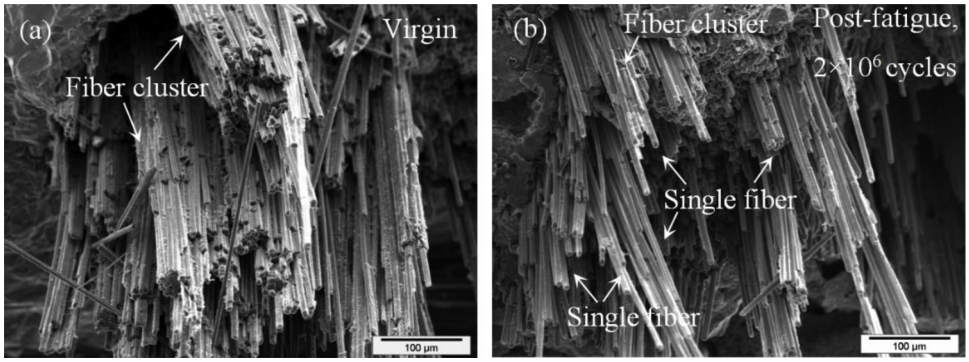

Fig. 7. SEM pictures of fracture surface of samples after quasi-static tensile test: (a) as-produced sample and (b) sample previously loaded with 2,000,000 fatigue cycles.

The damage evolution of the samples during the quasi-static tests, in terms of the cumulative A.E. hit count *vs*. the applied stress, are shown in Fig. 9. As it can be seen, the damage on the as-produced sample starts to increase at around 20 MPa, which is similar to the start of the non-linear part of the stress-strain curve (Fig. 8a). In addition, the damage develops with a constantly increasing rate (slope of the curve). Therefore, the measured damage threshold (see Table 3) does not represent correctly the onset in this case. On the other hand, the samples previously fatigue tested show only little damage at first, which rapidly increases after reaching the damage threshold. For the post-fatigue samples, the calculated damage threshold is indeed a good representation of the onset. Overall, the damage threshold increases with the number of fatigue cycles. The damage threshold of the sample after 200 cycles was still lower than the maximum fatigue stress applied, 55.8 MPa, while the other samples showed damage threshold above 58.2 MPa. It is also interesting to observe that the damage rate (slope of the curve) is different for each sample. In general, the damage rate decreases with the number of fatigue cycles previously applied.

4. Discussion

4.1. Damage analysis during fatigue loading

The damage analysis was performed by measuring the dynamic modulus and monitoring the A.E. signals (Fig. 4a). The reduction of the dynamic modulus is usually associated to the damage development on CMCs as it relates to the initiation and propagation of cracks in the matrix [20]. The increase of A.E. hits corresponds well with the decrease of the dynamic modulus, meaning that the amount of A.E. hits can also be related to the amount of damage in the composite. Hence, it

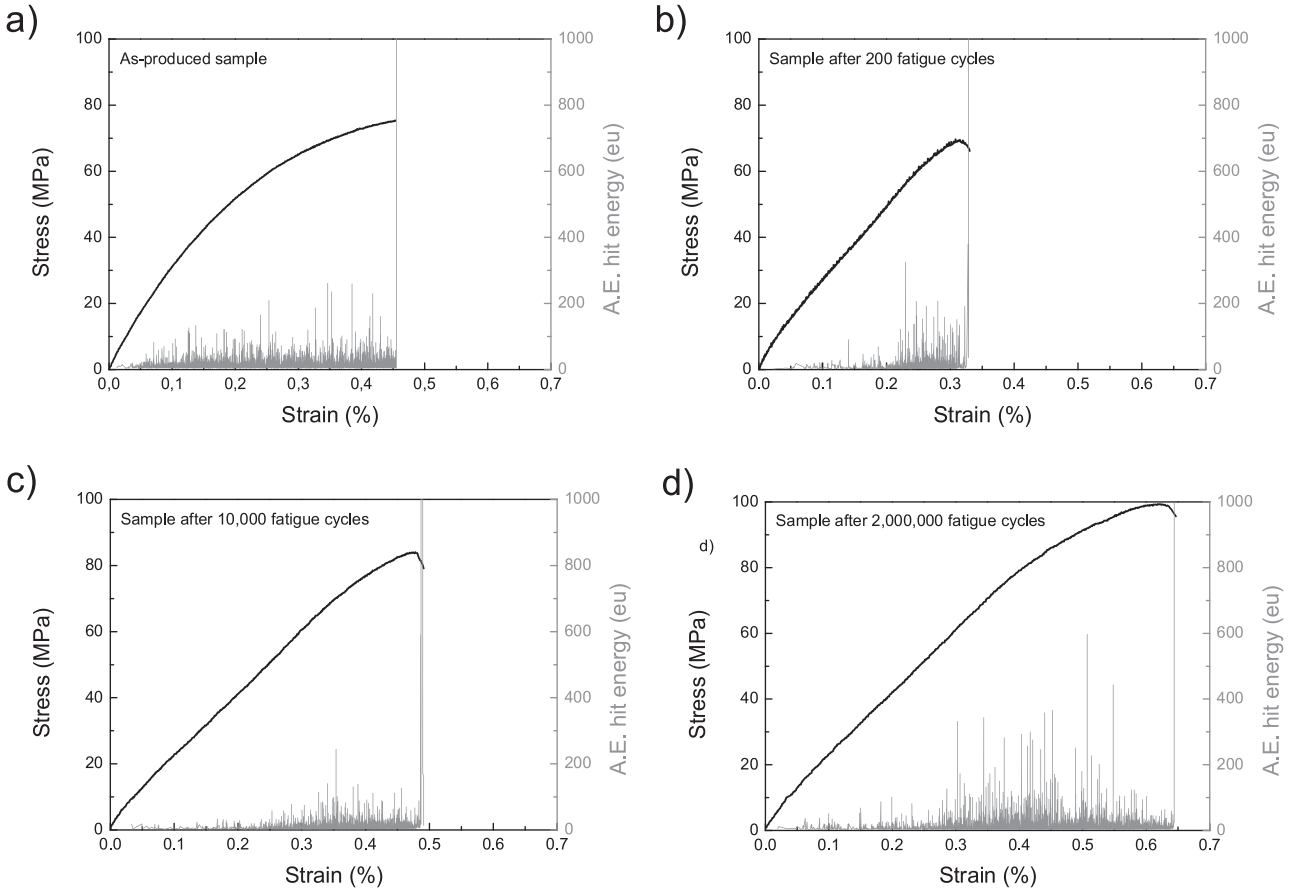

Fig. 8. Quasi-static tensile test of samples as-produced (a) and after 200 (b), 10,000 (c) and 2,000,000 (d) cycles with fatigue stress of 58.2 MPa.

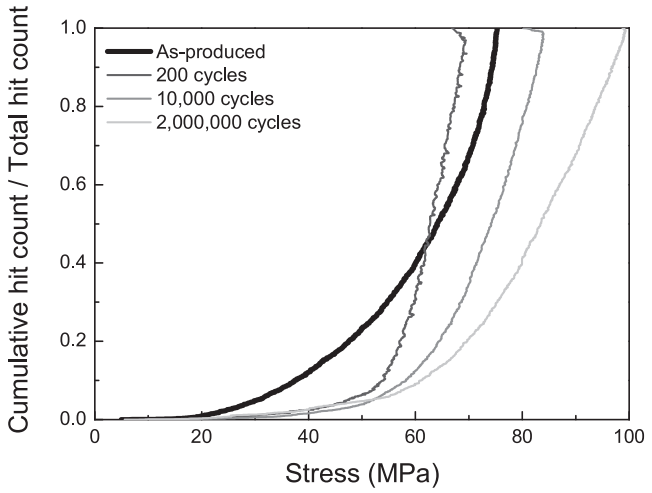

Fig. 9. Cumulative A.E. hit count *vs.* applied stress during quasi-static tensile loading on an as-produced sample and samples after fatigue loadings with fatigue stress of 58.2 MPa.

can be concluded that the damage generated during the first loading cycle is much higher than the subsequent ones. In general, the amount of new damage reduces with the number of cycles. Furthermore, this new damage will only occur at higher levels of stress (see Fig. 5). That means that the composite slowly approaches the saturation of matrix cracks related to the applied fatigue stresses. Therefore, it can be expected that the matrix cracks will eventually reach a stable state, at which no new considerable damage will occur in the matrix. This is not the case of the 200 cycles, as it can be seen in Fig. 6, i.e., the elastic modulus reaches a plateau only after 10,000 cycles.

In the literature, the A.E. energy is normally used for the quantification of damage [15]. As seen in Fig. 4a, however, the increase of A.E. energy follows a different trend than the decrease of dynamic modulus or the increase of A.E. hits. Some authors have proposed that the measured A.E. energy can be related to the type of damage mechanism that takes place [16,21]. Due to the complexity of the 2.5D composite tested (see Figs. 1 and 2), various types of damage including matrix crack initiation, matrix crack propagation, matrix crack re-opening, short fiber-matrix debonding, long fiber-matrix debonding and fiber breakage are expected to occur. Each of these damage mechanisms accumulate/release a different amount of energy. Therefore, the measured A.E. hit energy will depend not only on the amount of damage, but also on the type of loading and, most importantly, the type of damage. As previously mentioned, a much higher amount of A.E. hits was measured during the first cycle (Fig. 4a). In addition, the energy of the hits from the first cycle was considerably higher than the hits of the subsequent cycles (Fig. 4b). It is here suggested that those events measured within the first cycle are due to matrix crack initiation and propagation. The subsequent cycles show hits with lower energy, probably caused by crack propagation, with a few cycles showing hits over 200 eu, possibly more crack initiation. After 100 cycles, most of the A.E. hits present very low energy. In this stage, the low-energy A.E. activity corresponds to matrix crack re-opening. Hence, only a small amount of new damage occurs (Fig. 4a). Still, some cycles showed hits with higher energy, which can be related either to more crack initiation/propagation or to fiber matrix debonding. The propagation of cracks in the region of the short fibers and 0° long fibers, as well as fiber-matrix debonding caused by fatigue loadings were observed in our previous work [10]. This debonding is caused not only by the propagation of matrix cracks, but also by the friction between fiber and matrix during the cyclic loading-unloading. This friction constantly increases with the number of cycles. Therefore, fiber-matrix debonding can also happen at lower levels of stress, which explain the lower damage threshold seen for those cycles (Fig. 5).

4.2. Post-fatigue behavior

In order to discuss the post-fatigue behavior of the 2.5D C/C-SiC, it is important to understand the mechanical response of the as-produced composite. The as-produced sample showed a non-linear, quasi-plastic behavior (Fig. 8a), which is characteristic of CMCs that show crack deflection mechanisms. The increase of A.E. activity starts at around 20 MPa (Fig. 9), which coincides with the start of the non-linear part. In general, the A.E. signals show very similar energy in the beginning of the test, which indicates that the same type of event is happening. The fracture surface of as-produced samples consisted mainly of clustered fibers and little sign of fiber debonding (Fig. 7a). Therefore, it is safe to assume that most of the A.E. signals measured up to the maximum load are due to matrix crack initiation and propagation. The few signals with higher energy are probably caused by short fiber debonding, as well as the formation of the fiber clusters. At the end of the test, the load is high enough to cause the failure of the 0° long fibers. Hence, high-energy signals are measured at the moment of maximum load (Fig. 8a).

After the fatigue loading, an increase of the quasi-static tensile strength was seen (Fig. 6). This has also been observed on different CMCs in the literature, and it is normally related to the relief of internal stresses and reduction of the fiber-matrix interface strength [14,22]. On the other hand, the matrix cracking reduces the elastic modulus until reaching a state of stability, which depends on the fatigue stress. This state of matrix crack saturation is presumably reached after approximately 10,000 cycles for the fatigue stress of 58.2 MPa. Therefore, the sample that underwent only 200 cycles still showed non-linearity at stresses lower than the fatigue stress (Fig. 8b). Still, the A.E. activity was very low below the fatigue stress, being related to matrix crack re-opening and propagation. Considerable new damage starts to take place at around 55.8 MPa, i.e., damage threshold. The fact that the damage threshold is lower than the maximum fatigue stress previously applied is also an indication that the material did not reach saturation during the fatigue loading. The A.E. activity rapidly increases after reaching the damage threshold. Considering that after only 200 cycles the composite did not reach the saturation of matrix cracks and relief of internal stresses, the previous fatigue damage can increase the stress intensifications inside the composite. This leads to high-energy A.E. signals and earlier failure of the composite. This effect can also be seen in the damage rate (Fig. 9), i.e., when the material is loaded above the damage threshold, the damage increase is much faster than the other samples.

The relief of internal stresses starts to play a role in the mechanical response of the samples that reached matrix crack saturation. As previously discussed, these samples are the ones that underwent more than 10,000 cycles (see elastic modulus measurement in Fig. 6). Due to the relief of internal stresses [10], the measured A.E. signals show lower energy for the sample previously loaded with 10,000 cycles (Fig. 8c). In addition, the damage rate (Fig. 9) is much slower than the sample previously loaded with 200 cycles. This is also an indication that the stress concentrations are lower. When analyzing the sample with 2,000,000 cycles, it is clear that another type of damage takes place since this sample shows A.E. signals with much higher energy before the maximum load (Fig. 8d). The fracture surface analysis (Fig. 7b) showed clear signs of fiber debonding for this sample. This is an indication that interfacial degradation was caused by the fiber/matrix friction during the long-term cyclic loading. Hence, it can be concluded that the A.E. hits with higher energy are related to the debonding of long fibers. This type of event dissipates much more energy than matrix cracking or short fiber debonding. Due to this energy dissipation, the generation of new damage is hindered and the damage rate is slower than the other samples (Fig. 9). This also explains the extended non-linear region above the fatigue stress (Fig. 8d) and the increase of tensile strength (Fig. 6). Still, it should be highlighted that the steady increase of fiber-matrix friction will eventually lead to degradation of the material strength [10,14]. However, this was not clearly observed

in this work, even for the specimen loaded with 2,000,000 cycles.

5. Conclusion

Within this work, A.E. monitoring was successfully applied to analyze the damage evolution caused by cyclic and quasi-static loadings on 2.5D C/C-SiC composites. A.E. signals were measured during the first 200 cycles of a fatigue test with maximum stress of 58.2 MPa. In addition, the post-fatigue properties of the composite were characterized by quasi-static tensile tests with damage analysis on samples that survived different amounts of fatigue cycles. In summary, A.E. proved to be a powerful tool for the damage analysis as it provides information about the amount (number of A.E. hits), type (A.E. energy) and onset (damage threshold) of damage.

A.E. monitoring on the first 200 fatigue cycles showed that the generation of new fatigue damage rapidly decreases as the number of cycles increases. At the beginning of the test, the damage in the composite is related to matrix crack initiation and propagation. Later on, most of the A.E. signals measured were caused by matrix crack re-opening, and new damage occurred only near to the maximum fatigue stress. Still, new damage was also generated at lower stresses during some later cycles. In this case, the new damage is related to matrix crack propagation and fiber-matrix friction.

Further information on the possible damage mechanisms could be obtained by A.E. monitoring during the quasi-static tensile tests on samples before and after the fatigue tests. Based on our observations, the following damage mechanisms that can occur during loading are listed (in order of A.E. energy): matrix crack re-opening, matrix crack propagation, matrix crack initiation, short fiber debonding, long fiber debonding and fiber breakage. During the test on the as-produced sample, an extended region of non-linearity was observed and related to the increase of damage due to matrix crack initiation, propagation and crack deflection on the short fiber region. For samples that were previously fatigue loaded, a more linear behavior was observed. In summary, samples subjected to more fatigue cycles showed higher damage threshold and lower damage rate during the quasi-static tensile test. In addition, the specimen after 2,000,000 cycles also showed signs of long fiber debonding. Hence, an overall increase of the tensile strength was observed after the fatigue loadings, although a decrease of the elastic modulus was also observed.

Acknowledgements

Yang Li would like to express heartfelt gratitude to Dr. F. Reichert, Dip. W. Freudenberg and Dip. T. Liensdorf in Ceramic materials engineering (CME), University of Bayreuth and Mr. A. Mainz in Neue Materialian Bayreuth, Germany, for their kind support and assistance in mechanical tests. Additionally, the authors from China gratefully acknowledge the financial supports from National Key Research and Development Program of China (2016YFB0301403), the National Natural Science Foundation of China (Grant No. 51604107) and the Natural Science Foundation of Hunan Province of China (Grant No. 2019JJ50768 and 2019JJ50115).

References

[1] W. Krenkel, Carbon fiber reinforced CMC for high-performance structures, Int. J. Appl. Ceram. Technol. 1 (2) (2004) 188–200.
[2] R. Naslain, Design, preparation and properties of non-oxide CMCs for application in engines and nuclear reactors: an overview, Compos. Sci. Technol. 64 (2) (2004) 155–170.
[3] W. Krenkel, F. Berndt, C/C–SiC composites for space applications and advanced friction systems, Mater. Sci. Eng. A 412 (1–2) (2005) 177–181.
[4] P. Xiao, Z. Li, X. Xiong, Microstructure and tribological properties of 3D needle-punched C/C–SiC brake composites, Solid State Sci. 12 (4) (2010) 617–623.
[5] Z. Li, Y. Long, Y. Li, Li J-w, X. Xiong, P. Xiao, Microstructure and properties of needle punching chopped carbon fiber reinforced carbon and silicon carbide dual matrix composite, Ceram. Int. 42 (8) (2016) 9527–9537.
[6] S. Fan, L. Zhang, Y. Xu, L. Cheng, J. Lou, J. Zhang, et al., Microstructure and properties of 3D needle-punched carbon/silicon carbide brake materials, Compos. Sci. Technol. 67 (11) (2007) 2390–2398.
[7] Y. Wang, H. Wu, Microstructure of friction surface developed on carbon fibre reinforced carbon–silicon carbide (Cf/C–SiC), J. Eur. Ceram. Soc. 32 (12) (2012) 3509–3519.
[8] Z. Li, P. Xiao, B.-g Zhang, Y. Li, Y.-h. Lu, Preparation and tribological properties of C/C–SiC brake composites modified by in situ grown carbon nanofibers, Ceram. Int. 41 (9, Part B) (2015) 11733–11740.
[9] Z. Li, P. Xiao, Zhang B-g, Y. Li, Lu Y-h, S.-h. Zhu, Preparation and dynamometer tests of 3D needle-punched C/C-SiC composites for high-speed and heavy-duty brake systems, Int. J. Appl. Ceram. Technol. 13 (3) (2016) 423–433.
[10] Y. Li, P. Xiao, H. Luo, R.S.M. Almeida, Z. Li, W. Zhou, et al., Fatigue behavior and residual strength evolution of 2.5D C/C-SiC composites, J. Eur. Ceram. Soc. 36 (16) (2016) 3977–3985.
[11] Y. Li, P. Xiao, Y. Shi, R.S.M. Almeida, W. Zhou, Z. Li, et al., Mechanical behavior of LSI based C/C-SiC composites subjected to flexural loadings, Compos. Part A Appl. Sci. Manuf. 95 (2017) 315–324.
[12] B.F. Sørensen, J.W. Holmes, E.L. Vanswijgenhoven, Rate of strength decrease of fiber-reinforced ceramic-matrix composites during fatigue, J. Am. Ceram. Soc. 83 (6) (2000) 1469–1475.
[13] K.G. Dassios, D.G. Aggelis, E.Z. Kordatos, T.E. Matikas, Cyclic loading of a SiC-fiber reinforced ceramic matrix composite reveals damage mechanisms and thermal residual stress state, Compos. Part A Appl. Sci. Manuf. 44 (2013) 105–113.
[14] G. Fang, X. Gao, S. Zhang, J. Xue, Y. Song, F. Wang, A residual strength model for the fatigue strengthening behavior of 2D needled CMCs, Int. J. Fatigue 80 (2015) 298–305.
[15] G.N. Morscher, Stress-dependent matrix cracking in 2D woven SiC-fiber reinforced melt-infiltrated SiC matrix composites, Compos. Sci. Technol. 64 (9) (2004) 1311–1319.
[16] M. Bourchak, I.R. Farrow, I.P. Bond, C.W. Rowland, F. Menan, Acoustic emission energy as a fatigue damage parameter for CFRP composites, Int. J. Fatigue 29 (3) (2007) 457–470.
[17] E. Volkmann, A. Dentel, K. Tushtev, C. Wilhelmi, K. Rezwan, Influence of heat treatment and fiber orientation on the damage threshold and the fracture behavior of Nextel fiber-reinforced Mullite-SiOC matrix composites analysed by acoustic emission monitoring, J. Mater. Sci. 49 (22) (2014) 7890–7899.
[18] R.Y. Kim, N.J. Pagano, Crack initiation in unidirectional brittle-matrix composites, J. Am. Ceram. Soc. 74 (5) (1991) 1082–1090.
[19] M. Surgeon, E. Vanswijgenhoven, M. Wevers, O. Van Der Biest, Acoustic emission during tensile testing of SiC-fibre-reinforced BMAS glass-ceramic composites, Compos. Part A Appl. Sci. Manuf. 28 (5) (1997) 473–480.
[20] B.F. Sørensen, J.W. Holmes, E.L. Vanswijgenhoven, Does a true fatigue limit exist for continuous fiber-reinforced ceramic matrix composites? J. Am. Ceram. Soc. 85 (2) (2002) 359–365.
[21] M. Wevers, I. Verpoest, P. De Meester, Identification of fatigue failure modes in carbon fibre reinforced composites, in: J. Boogaard, G.M. van Dijk (Eds.), Non-Destructive Testing, Elsevier, Oxford, 1989, pp. 459–465.
[22] H. Mei, L. Cheng, Stress-dependence and time-dependence of the post-fatigue tensile behavior of carbon fiber reinforced SiC matrix composites, Compos. Sci. Technol. 71 (11) (2011) 1404–1409.